Solar Energy Advances 1 (2021) 100009

Contents lists available at ScienceDirect

Solar Energy Advances

journal homepage: www.elsevier.com/locate/seja

On the winter overcooling penalty of super cool photonic materials in cities

Ansar Khan[a], Laura Carlosena[b,*], Samiran Khorat[c], Rupali Khatun[d], Quang-Van Doan[e], Jie Feng[f], Mattheos Santamouris[f]

[a] Department of Geography, Lalbaba College, University of Calcutta, Howrah, WB 711202, India
[b] Department of Engineering, Public University of Navarra (UPNA), Arrosadia Campus, 31006 Pamplona, Spain
[c] Department of Geography, University of Calcutta, Kolkata, WB 700019, India
[d] School of Oceanographic Studies, Jadavpur University, Kolkata, WB 700 032, India
[e] Centre for Computational Sciences, University of Tsukuba, Ibaraki 305 8577, Japan
[f] Faculty of Built Environment, University of New South Wales, Sydney, NSW 2052, Australia

ARTICLE INFO

Keywords:
Broadband emitters
Overcooling
WRF-SLUCM
Kolkata
Daytime radiative coolers

ABSTRACT

Daytime radiative coolers appear to be the most triumphant and promising technology for urban thermal management, as they could improve the thermal field of the cities, especially during the summertime. However, during the colder months, it can lead to an overcooling penalty, a widely overlooked phenomenon. This study aims to determine the cooling penalty derived from using super-cool materials (SCMs) at a city scale. We used a mesoscale urban modeling system to assess the overcooling of three broadband SCM emitters with different reflectivity and emissivity values. A significant change was found in radiation and energy balance compared to the control case (CTRL) during the daytime and nighttime. Under the most reflective and emissive SCM scenario, the maximum decrease of net radiation at peak hour was 354.9 Wm^{-2}, therefore choosing a scenario with lower albedo values for walls and ground would be more beneficial. The mean decrease of ambient temperature, surface temperature, roof temperature and canopy were 2.8 °C, 4.7 °C, 12.9 °C and 6 °C, respectively. This SCMs assessment is a first stride to understand better the unexplored behavior of the boundary layer meteorology and its depiction in the mesoscale climate model for winter seasons. The implementation of SCMs during winter could create an inversion layer near the surface, leading to a buildup of stagnant air over the urban environment, resulting in heating during the night in the winter seasons as usual with SCMs as with the CTRL. Further research is needed on material development to modulate materials' spectral configuration to address overcooling during the winter and improve SCMs' year-round performance at city scale.

Introduction

Cities run the risk of becoming victims of their own success and causing ever-larger global ecological footprints and urban environmental externalities. Haphazard urban growth is a seemingly unbeatable global process in the major cities. Thus, rapid urbanization around the globe is exacerbating the amount of land converted to urban land, resulting in increased surface and ambient temperatures in those areas [33, 42]. Urban overheating is related to higher urban temperatures in dense parts of cities caused by the positive thermal balance of the urban regions in comparison with their surrounding rural areas [2]. Moreover, urbanization can induce phenomena such as the urban dryness island referring to conditions where lower humidity values are observed in cities relative to more rural locations, and to slower wind speed compared to adjacent suburbs and countryside [20].

Oke et al. identified as the most prevalent causes of urban heating the significant release of anthropogenic heat, the excess storage of solar radiation by city structures, the lack of green spaces and cold sinks, the non-circulation of air in urban canyons, and the reduced ability of emitted infrared radiation to escape into the atmosphere [43]. A total of 400 cities worldwide have been identified to suffer from this phenomenon called the urban heat island (UHI), and the number of cities is increasing rapidly [51]. Moreover, heat islands are related to amplified cooling loads, health risks, and vulnerability during the summer [62] as the rise of the peak electrical load per degree of ambient temperature increase varies between 0.45% and 4.6% [52].

Furthermore, heatwaves intensify UHI both during day and night [15] and severely impact thermal comfort, cooling energy consumption, the concentration of harmful pollutants, and heat-related mortality and morbidity [50]. Recent research has found that populations living in cities with warmer precincts have a close to 6% higher mortality risk than those living in cooler urban neighborhoods [57]. In the context of

* Corresponding author.
E-mail address: laura.carlosena@unavarra.es (L. Carlosena).

https://doi.org/10.1016/j.seja.2021.100009
Received 23 September 2021; Received in revised form 7 November 2021; Accepted 8 November 2021
Available online 10 November 2021

Nomenclature

$T_{ambient}$	Ambient temperature
$T_{surface}$	Surface temperature
T_{air}	Air temperature
T_{canopy}	Urban canopy temperature
T_{roof}	Roof surface temperature
Q_*	Net inflow radiation
Q_E	Latent heat flux
Q_H	Sensible heat flux
Q_G	Heat storage
SCM	Super cool material
DRC	Daytime radiative coolers
KMA	Kolkata metropolitan area
PBL	Planetary boundary layer
WRF	Weather research and forecasting
SLUCM	Single layer urban canopy model
SUHI	Surface urban heat island
IMD	India Meteorological Department
UCM	Urban canopy model
CTRL	Control case
CAPE	Convective available potentian energy

regional climate change, heatwaves are more frequent, intensified, and prolonged, which coupled with rapid urbanization aggravate thermal risk in urban environments. To counterbalance the continuous increase of the amplitude of urban heat and the frequency and magnitude of heatwaves, efficient urban mitigation and adaptation policies involving natural and artificial cooling technologies have to be developed and implemented [55]. The potential mitigation measures to counterbalance the impact of climatic change in the cities are urgent. To offset the impact of urban warming, numerous large-scale mitigation technologies have been proposed. For decades, reflective rooftops with white coatings have been used and advocated as cost-effective measures to mitigate the urban heat and reduce building cooling loads [1, 6, 25, 24, 49, 54].

The recent technological progress has resulted in material developments with engineered spectral properties such as IR reflective particles, phase change materials (PCM) [10, 48], thermochromic materials [23, 45, 68], fluorescent materials [16, 26], photonic [5, 31, 30] and plasmonic materials [39]. In addition, urban heat mitigation solutions can be achieved by cutting off incoming solar radiation with broadband radiative coolers. New building materials can reduce urban temperatures and counteract the effects of local climate change. These technologies could turn building environments into climate-fighting tools.

Radiative coolers or super cool materials (SCMs) have raised researchers' interest in the last years due to their high mitigation potentials [60]. These materials rely on increasing a natural heat-shedding effect, known as the passive radiative cooling process. Radiative cooling is the physical phenomenon by which an object dissipates heat as infrared radiation through the atmospheric transparency window, over mid-infrared wavelengths, between 8 and 13 μm [34]. The optical properties of SCMs fall into two categories: strictly selective materials (highly emissive only in the atmospheric window) and broadband materials (highly emissive in the infrared range). These materials have achieved albedo and emissivity values greater than 0.96 and 0.97, respectively. A high broadband emittance SCM is preferred for above ambient cooling. Broadband emitters exhibit better performance in arid climates, being detrimental under humid climatic conditions [13, 19]. As a result, broadband radiators enhance radiative cooling in the daytime yet suppress overcooling at night, leading to a narrowed diurnal temperature difference than the selective emitter. Such a difference can be attributed to the broadband radiator's stronger heat exchange capacity with the sky [64]. As a result, the daytime radiative broadband emitters end up absorbing greater atmospheric radiation.

Recent studies reported that SCM surfaces could radiate away enough heat to consistently stay up to 5–10 °C cooler than the surrounding ambient air temperature, even under the typical mid-summer day due to their high solar reflectivity and high infrared emissivity [14, 29, 67]. A comparison of several mitigation techniques on an urban street canyon concluded that, on its own, radiative cooling materials applied on shading devices decreased up to 1.6 °C ambient temperature and 24.2 °C surface temperature, being one of the most efficient strategies in the study [4]. The main limitations with the broad application of SCMs are the costly material fabrication and scalability [12, 53, 65, 66]. However, current efforts are directed towards achieving easy to develop and apply materials. For example, a recent study developed a low cost (0.3 €/m^2 for a layer of 2 μm of PMSQ and SiO_2 particles), scalable and sprayable SCM able to reduce the bare substrates' temperature under non-ideal climatic conditions 1.7 °C with up to 12 °C temperature drops [7].

Besides using SCMs as passive cooling materials, they might be used for electricity generation at night, water condensation during the day, and reduce the demand for power-hungry refrigeration and air conditioning [47, 56]. In addition, super cool roofs and pavements reduce the energy needed for cooling. As a result, their implementation decrease CO_2 emissions that increase the magnitude of climate change. Thus, making cities more economical, environmentally friendly, and liveable. However, few studies have considered these materials as part of a geoengineering strategy to help the earth shed heat to offset global rising temperatures rather than block the sun's incoming energy [41]. Moreover, SCMs might not endure all weathers or be easily adapted for all building morphologies and environments. Through the modulation of reflectivity and emissivity of the materials, SCMs can have the capacity to both cool the urban environment in summer and heat in winter. These materials can reflect, refract, and form interference patterns, which can positively, negatively, or synergistically impact urban environments.

The urban cooling effect works preeminently in dry climates and with a calm atmosphere during summer. The cooling potential of radiative coolers reduces significantly in high humidity zones as high atmospheric water vapor concentration reduces the transmissivity in the atmospheric window wavelengths (8–13 μm). Thus, water vapor traps a significant amount of infrared radiation from the urban surface under cloudy or humid weather, preventing heat exchange with outer space.

Despite the mounting comprehension of urban heat mitigation technologies, the numerical assessments of recently developed innovative SCMs broadband emitters are scarce. SCMs were simulated for the first time at a city scale in the city of Kolkata, achieving excellent results; being able to reduce the peak air temperature in a city from 5.3 °C to 1.6 °C, depending on the scenario [14]. Moreover, results reported that broadband coolers could significantly mitigate summertime urban heat. However, the cooling island effect they generate would increase side effects such as a decrease in the mixing layer of the lower atmosphere and an augment in pollutant deliberation. The use of SCMs might increase the energy savings but might increase the heating energy penalty compared with a cool roof [3, 17]. To our understanding, there is a substantial lack of scientific investigation on the performance of reflective materials for a tropical wet and dry climate and the associated meteorological effects at a city scale. While in most cities the surrounding environment is at a lower temperature, generating advective flows advantageous for the urban zones, coastal cities are surrounded by much cooler environments causing the urban cooling passively of these cities through sea breeze and affecting the regional thermal balance in an utterly diverse way than the land locked cities. Therefore, studying the impact of SCMs as a well-liked approach of urban mitigation strategies for urban heat management in tropical regions is imperative. To do so, a high-resolution city scale model is used to test the cooling efficiency of the SCMs materials, assess the city's thermal balance, and determine the best solution for future urban sustainability. The different SCMs scenarios were simulated under a well-validated model during the wintertime for Kolkata Metropolitan Area (KMA). It is expected that the implemen-

tation of advanced mitigation technologies, such as the implementation of SCMs, will significantly reduce the buildings' energy consumption, enhance thermal comfort, social equity and improve heat-related health issues in the cities rather than excess overcooling for the winter season. The primary questions to be addressed through this study are:

a) How can SCMs endorse the urban thermal environment in tropical cities, and which materials perform best for the winter season?
b) What is the overcooling penalty under a choice of modified albedo environment in tropical cities during winter?
c) What are the lower atmospheric effects caused by the alteration of the urban albedo in tropical cities during the cold period?

Thus, this study aims to determine the winter overcooling penalty of super cool photonic materials in cities. We forecasted the impact on an urban scale of different types of broadband SCMs during the cold season. The sensible heat, latent heat, heat storage, and net inflow radiation were calculated alongside the ambient temperature, the roof temperature, and the urban canopy temperature (both day and night).

Methods

Climate and location selection

For this study, simulations were carried out during clear sky and calm wind situations during two consecutive days around the winter solstice in Kolkata, from the 21st of December to the 22nd of December 2019. Three scenarios plus one control case (CTRL), were simulated in a tropical wet and dry climate (Aw-Tropical Savanna Climate under the Köppen Geiger classification scheme). During the selected period, the maximum and minimum temperatures were 24.2 °C and 14.5 °C, respectively, with average values of 20.1 °C. The average relative humidity was 57.8% and the observed average UHI was 3.1 °C with maximum values of 5.6 °C and minum of 0.6 °C. The KMA was selected as previous research [14] has shown it would benefit from SCMs during the summer. Thus, the impact in winter was assessed in the same location. Moreover, KMA is considered a representative location of the regional tropical context.

Model configuration

In this research, the community Weather Research and Forecasting (WRF v4.0.0) model was coupled with a highly sophisticated single-layer urban canopy model (SLUCM) [27]. As shown in Fig. 1, we configured WRF-SLUCM over a one-way parent domain D01 (black) (22.57°N, 88.36°E) with a horizontal grid resolution of 18 km and two nested domains: D02 (blue) with 6 km resolution, and D03 (red) centered in Kolkata city with a 2 km resolution. The figures' background shows the topography of Kolkata metropolitan areas (KMA). The default parameter values for the urban table were used in the WRF-SLUCM model.

The initial and boundary meteorological conditions of the WRF-SLUCM were defined based on the high-resolution National Centers for Environmental Prediction (NCEP) Global Forecasting System (GFS) Operational Global Analysis and Forecast Datasets (NCEP-GFS 0.25 Degree Global Forecast Grids, 2015). The resolution of the grid is 0.25 by 0.25° and is prepared for every three hours up to 240 h. In addition, several models were included for the physical parameterization of the WRF model: the rapid radiative transfer model [38] for longwave radiation, the Dudhia scheme [11] for shortwave radiation, the Mellor and Yamada's TKE scheme [37] for the Turbulence, the Purdue-Lin scheme [32] for the microphysics, the Asymmetrical Convective Model version 2 [46] for the planetary boundary layer, Kain-Fritsch (KF) scheme [22] for cumulus parameterization and the Noah-LSM with single-layer urban canopy model [9, 27] was implemented as the model surface layer.

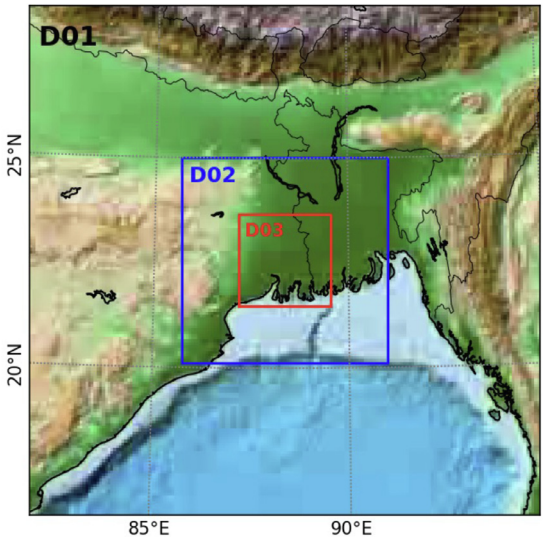

Fig. 1. The three domains setup adopted for WRF in the current study, showing the model topography in colours.

Model validation and evaluation

The performance of the WRF-SLUCM model was evaluated by comparing the base case simulation with local observations over the D03 domain urban grid cell, using the hourly output of the air temperature at 2-m high for two consecutive days. These two days were the coldest in 2020, as per India meteorological department (IMD) records. The hourly climate data were obtained from six local meteorological stations from Kolkata Municipal Corporation (joint venture of Indian Institute of Technology Kharagpur and Kolkata Municipal Corporation) to evaluate and validate the model.

Table 1 presents the statistical comparison of the mean bias error (MBE), mean absolute error (MAE), root mean square error (RMSE), and correlation coefficient (r) for the hourly 2-m air temperature.

The base case simulation agreed soundly with local observations ($p<0.05$) and forecasted urban conditions well. In addition, the WRF-SLUCM model could accurately forecast the temperature observed at different stations with a 0.89 correlation coefficient and 0.81 mean bias error. The mean bias error of air temperature ranges from −0.5 °C to 2.1 °C, and the root means square error, from 0.8 °C to 2.9 °C. Ratan Babughat (RBG) obtains the most accurate estimates of 2-m air temperature over the urban grid, 0.8 °C. Uncertainties of the model parameters, physical schemes, input data, and lack of proper urban morphological representation are the most probable causes of model biases. In this case and most likely due to an error in the solar radiation over the urban domain, the model slightly underestimates the 2-m air temperature.

Nevertheless, the index of agreement ranges from 0.81 to 0.95 compared to the simulated result. Thus, the presented validation proved that the WRF-SLUCM model could reproduce the urban environment realistically. As a result, the model could be used for future research related to other mitigation strategies for urban heating.

Study cases: Kolkata metropolitan area

The performance of SCM broadband emitters was evaluated with the hourly simulation data of the model innermost domain (D03), excluding the first 24-h of the simulation from post-processing and analysis as they were the model spin-up time. This area is considered as a core urban region in KMA within our study domain.

One CTRL and three additional numerical experiments were conducted in this study to evaluate the performance of SCMs as urban heat mitigation technologies. In addition, the CTRL simulation with default urban parameters is set up to verify the reliability of the model by com-

Table 1
Simulation results comparison with observed data.

Parameters	Local meteorological stations					
	Alipore (ALP)	Ratanbabu Ghat (RBG)	Shibpur (SHP)	Palmer Bridge (PLB)	Jora Bridge (JRB)	Joka (JKA)
Correlation coefficient	0.8165	0.9687	0.9422	0.8634	0.8216	0.9326
Mean bias error	−2.1	−0.34	−0.89	−1.0	0.05	−0.54
Mean absolute error	−2.10	−0.33	−0.88	−1.02	0.04	−0.54
Root mean square error	2.9	0.80	1.40	1.90	2.00	1.40
Index of agreement	0.81	0.98	0.95	0.90	0.89	0.95

Table 2
Numerical design of WRF-UCM simulation for SCM broadband emitters in winter case.

Numerical design	Type of roof	Mitigation strategies (urban areas)	
		Albedo fraction	Emissivity fraction
Control case (CTRL)	Conventional roof	Roof 0.20 Wall 0.20 Ground (road) 0.20	Roof 0.90 Wall 0.90 Ground (road) 0.95
Super cool materials-A (SCMs-A)	Super cool roof	Roof 0.96 Wall 0.91 Ground (road) 0.71	0.97 for All
Super cool materials-B (SCMs-B)	Super cool roof	Roof 0.96 Wall 0.30 Ground (road) 0.40	0.97 for All
Super cool materials-C (SCMs-C)	Super cool roof	Roof 0.90 Wall 0.20 Ground (road) 0.20	0.90 for All

paring the simulation results and observation data collected from local weather stations. The different scenarios have different albedo and emissivity values for roofs, walls, and grounds (Table 2). The modification of albedo and emissivity on the building façade and urban surface can change the energy balance of the city. Increasing the albedo and emissivity fraction in urban grid cells can modify the energy component of fluxes of urban surfaces.

The SCMs are highly reflective in the solar wavelengths (more than common materials), as a result, they are relatively unaffected by incoming solar radiation. On the other hand, common reflective materials (white paint and cool-colored paint) have a consistent emissivity in the whole longwave electromagnetic spectrum. On the contrary, SCMs have varying spectral emissivity. The current version of WRF-UCMs (single layer or multilayer) does not allow the wavelength-dependent emissivity values in the urban parameter table of the WRF urban modeling system. Therefore, the albedo and emissivity of all the urban surfaces were modified from 0.2 (CTRL simulation) to 0.96 and 0.90 to 0.97, respectively. One CTRL and three additional scenarios considering higher albedo values were designed and simulated as well. In the three modified albedo scenarios, we considered increasing the initial albedo value from 0.20 (CTRL simulation) to 0.96 over Kolkata city. An albedo close to 0.20 can be achieved using commercially available conventional materials at a city scale; it is considered a realistic research assumption. The three other scenarios consider high albedo values at the upper limit of the commercial technological solutions. The wall, roof, and ground albedo were changed for SCMs-B and SCMs-C, and they are considered reasonable values according to the current mitigation technology [14]. A high albedo wall value of 0.91, such as in SCMs-A, may affect car drivers and pedestrians as the reflected light might glare and have contrast effects. However, given the rapid development of the so-called super cool photonic materials presenting reflectance values above 0.90, it is of particular interest to explore the cooling potential and the impact on the atmospheric dynamics of such high albedo values at the city scale during the extreme winter period

Results of the city scale simulations

For all scenarios described in Table 2, net inflow radiation Q_*, latent heat Q_E, sensible heat Q_H, and heat storage Q_G, were calculated and comparatively discussed. The results of the simulations are summarized in Table 3. Fig. 2 shows the alterations in heat flux components over urban environments in the different scenarios and compared to the CTRL. Results showed that each flux partition component significantly dropped when SCMs were applied on a city scale.

Table 3
Distribution of flux parameters for SCM broadband emitters in winter case.

Time	Flux parameter (Wm^{-2})	SCMs-A	SCMs-B	SCMs-C
Daytime	$Q_{H\ max}$	−186.8	−148.8	−128.7
	$Q_{H\ mean}$	−86.7	−68.2	−58.9
	$Q_{E\ max}$	−38.6	−16.2	−13.9
	$Q_{E\ mean}$	−18.1	−9.0	−7
	$Q_{G\ max}$	144	67.6	45.9
	$Q_{G\ mean}$	56.8	25.1	16.3
	$Q_{*\ max}$	−354.9	−220.2	−177.4
	$Q_{*\ mean}$	−161.6	−102.3	−82.2
Nighttime	$Q_{H\ max}$	−8.8	−4.9	−3.1
	$Q_{H\ mean}$	−7.7	−4.1	−2.7
	$Q_{E\ max}$	3.5	2.8	2.6
	$Q_{E\ mean}$	0.7	0.7	0.4
	$Q_{G\ max}$	−35.3	−19.1	−14.1
	$Q_{G\ mean}$	−25.9	−13.5	−10.1
	$Q_{*\ max}$	28.3	15.8	12.1
	$Q_{*\ mean}$	18.9	10.1	7.8

The maximum decrease of sensible heat ($Q_{H_{max}}$) occurred at peak hour, and the values ranged from 186.8 Wm^{-2} to 128.7 Wm^{-2}. Thus, the SCMs had the highest impact on Q_H reduction due to cut-off input radiation, and the input energy was lower over the urban domain. On the other hand, during nighttime, the average Q_H decrease was lower than daytime, varying from 7.7 Wm^{-2} to 2.7 Wm^{-2}. Thus, SCMs could reduce a daily average negative sensible heat from 20 Wm^{-2} to 40 Wm^{-2} compared to the CTRL.

The maximum decrease of latent heat ($Q_{E_{max}}$) occurred at peak hours as well. All scenarios SCMs-A, SCMs-B and SCMs-C decreased latent heat during the day. However, the reversed conditions occurred during nighttime, where latent heat increased for the three studied cases. Urban evaporative surfaces received a meager amount of solar energy due to the high reflection of incoming solar radiation during the daytime, so the latent heat reduction is comparatively low.

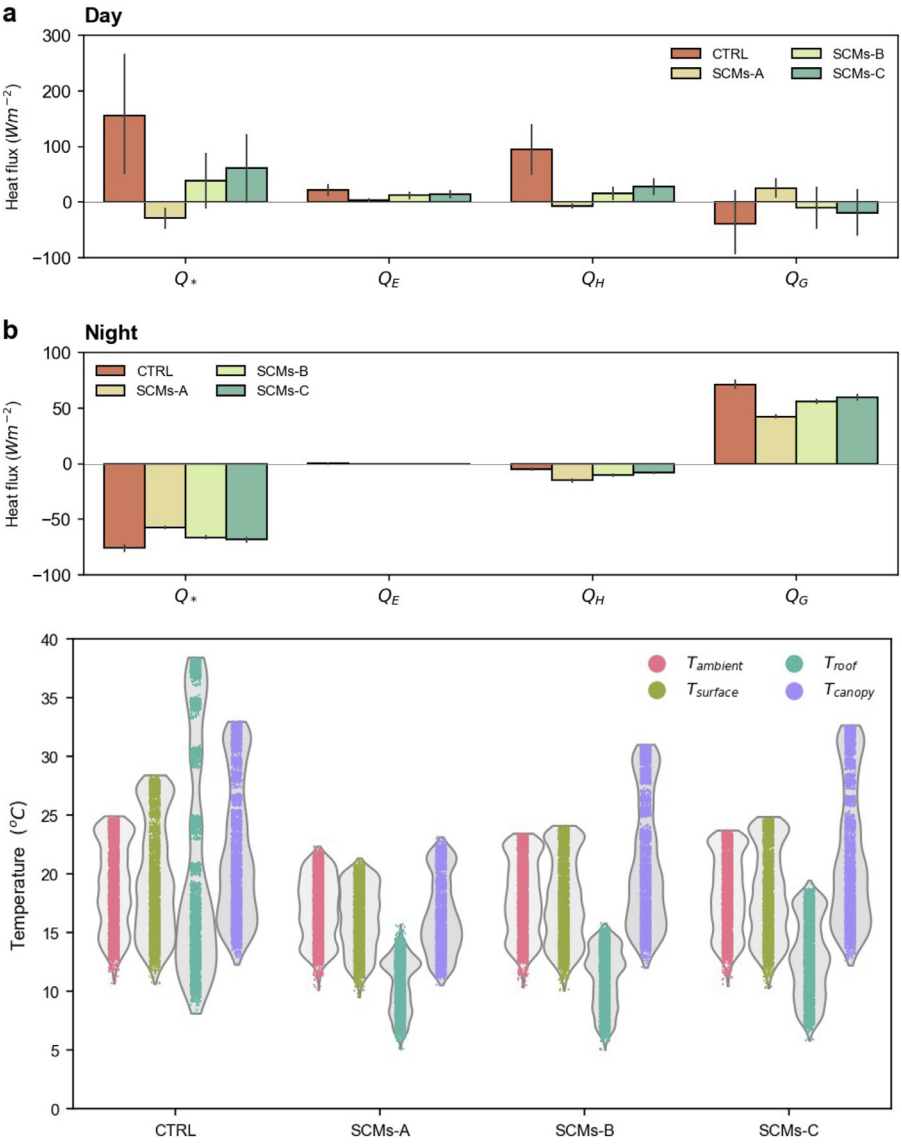

Fig. 2. WRF simulations of surface energy heat fluxes for a typical winter day episode with SCMs. Differences in heat fluxes derived from two-dimensional surface energy budget/radiation from WRF-SLUM model simulations.

Fig. 3. Violin plots of urban state variables (hourly) temperatures over the urban area where SCMs are implemented. Results of 24-h x169 points, whose albedo and emissivity were changed. The comparisons were done with the newly developed SCMs (SCMs-A, B, C) and CTRL for $T_{ambient}$, $T_{surface}$, T_{roof}, and T_{canopy}. These temperatures derived from the energy budget on the canyon surface of each facet (roof, wall, and ground) through their effect on the heat fluxes. WRF 2-m temperature was considered as $T_{ambient}$.

The SCMs mitigate urban overheating mainly by decreasing the solar radiation absorbed by the urban surfaces and reemission of the absorbed heat, so the net inflow radiation (Q_*) was also reduced during the daytime; as a result, the maximum decrease occurred at peak hours due to their high albedo values, especially for SCM-A with the highest roof, wall and ground numbers. The reverse phenomenon occurred at nighttime. Consequently, the maximum decrease of net radiation occurred at peak hour with values ranging from 354.9 Wm^{-2} to 177.4 Wm^{-2}.

Besides calculating the different heat fluxes, the ambient, roof, surface, and canopy temperatures were obtained from the surface energy balance flux partitions in the WRF-SLUCM urban modeling system (Fig. 3).

The results, summarized in Table 4, showed a reduction of the maximum ambient temperature ($T_{ambient\ max}$) for all SCMs scenarios, ranging from 4.2 °C to 1.6 °C. The minimum ambient temperature reduction ($T_{ambient\ min}$) also significantly varies for each case scenario (from 0 °C to 0.1 °C) during the simulation period depending on the albedo and emissivity fraction change. The diurnal profile of ambient temperature ($T_{ambient}$) reduction was also presented by the daytime and nighttime average of each super cool roof scenario with similar meteorological conditions. During the daytime, the highest average ambient temperature ($T_{ambient}$) reduction was 2.8 °C, achieved with SCMs-A. As mentioned before, SCMs-A has the highest overall albedo and emissivity values among the considered scenarios for roofs, walls, and ground.

Table 4
Distribution of temperature reduction in winter, comparison of the SCM broadband emitters with the CTRL.

Time	Thermal parameter (°C)	SCMs-A	SCMs-B	SCMs-C
Daytime	$T_{ambient\ max}$	−4.2	−2	−1.6
	$T_{ambient\ mean}$	−2.8	−1.2	−0.9
	$T_{surface\ max}$	−7.3	−4	−3.3
	$T_{surface\ mean}$	−4.7	−2.5	−2
	$T_{roof\ max}$	−21.2	−20	−16.9
	$T_{roof\ mean}$	−12.9	−12.1	−10.2
	$T_{canopy\ max}$	−9.3	−1.6	−0.5
	$T_{canopy\ mean}$	−6	−0.7	−0.2
Nighttime	$T_{ambient\ max}$	−2.4	−1.1	−0.7
	$T_{ambient\ mean}$	−1.5	−0.7	−0.5
	$T_{surface\ max}$	−2.9	−1.5	−0.9
	$T_{surface\ mean}$	−2	−1	−0.6
	$T_{roof\ max}$	−7.2	−6.3	−5
	$T_{roof\ mean}$	−5	−4.4	−3.5
	$T_{canopy\ max}$	−5.4	−0.9	−0.3
	$T_{canopy\ mean}$	−3.9	−0.7	−0.2

Moreover, SCMs-A's maximum reduction ambient temperature at nighttime is 2.4 °C with average values of 1.5 °C. Therefore, all the stud-

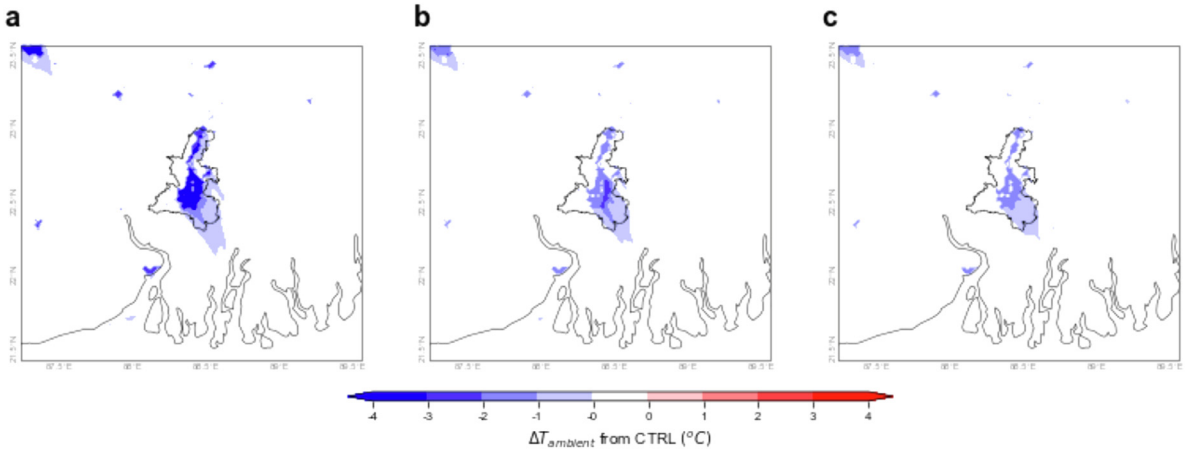

Fig. 4. Drop of $T_{ambient}$ compared to the CTRL. Results showed that temperature drops in DO3 for urban areas of KMA where SCMs are implemented. In this case (a) SCMs-A significantly drops the temperature due to high albedo of the materials and emissivity compared to (b) SCMs-B, and (c) SCMs-C.

ied scenarios could reduce the peak UHI intensity nevertheless, they would decrease thermal comfort during the winter days. The benefits of using the materials during the summer could compensate the heating penalty during the winter. As a result, the peak electricity demand would decrease during the summer but increase during the winter. Evidence suggests that for each degree of ambient temperature decrease, the corresponding peak electricity demand reduces between 0.45% and 4.6%; this equals an additional peak electricity benefit of 21 (±10.4) W/person of each degree temperature decreases [52].

SCMs-A achieved the highest ambient and surface temperature reduction since it has the highest albedo values for all the parameters (roof, wall, and ground) combined with the highest emissivity. As a result, SCMs-A's maximum surface temperature reduction was 7.3 ˚C during the daytime and 2.9 ˚C at night. The average surface temperature reduction for all scenarios during the day ranged from 4.7 ˚C to 2 ˚C with values from 2 ˚C to 0.6 ˚C at nighttime. Consistently, the highest urban canopy temperature reduction was for SCMs-A, 9.3 ˚C during the day and 5.4 ˚C at night, being almost negligible for SCMs-C (0.5 ˚C day and 0.2 night).

The maximum roof surface temperature ($T_{roof\,max}$) also decreased up to 21.2 ˚C with an average of 12.9 ˚C for SCMs-A with a maximum reduction of T_{roof} is 7.2 ˚C during nighttime. The average roof temperature decrease T_{roof} during nighttime is less than daytime, again SCMs-A achieved the highest reduction, 5 ˚C.

The CTRL thermal parameters difference is high enough compared to the reflective materials for all cases. These SCMs yield close to 100% solar reflection and thermal emittance at the atmospheric window (8 to 13 μm). Therefore, high spectral requirements at short and long wavelengths are required to achieve suitable SCMs for heat mitigation.

Similar to previous studies, we studied the roof temperature of different roof surfaces (SCMs roof) and compared it to CTRL simulation (conventional roof) as shown in Fig. 4. The conventional roof (CTRL) is 5.6 ˚C above the sub-ambient, while the SCMs roof remains 5.3 ˚C below the sub-ambient under peak solar radiation. Results confirm that excellent thermal performance is maintained through the SCMs implemented roof surface. The results also suggested that the roof temperature (T_{roof}) constantly remains below the ambient temperature ($T_{ambient}$) simulation due to negative flux at the diurnal scale released into the urban environment. The differences between $T_{surface}$ and $T_{ambient}$ were 1.1 ˚C, 0.7 ˚C, and 0.6 ˚C, respectively for each scenario. The intensity of heat reduction is high during peak solar energy. High albedo and emissivity do not create contrast and glare during peak temperature in the urban atmosphere in SCMs-A in winter. The absorption of the atmospheric radiation largely depends on local energy balance, convection, atmospheric water, synoptic weather conditions, and building morphologies within the city domain during winter.

The intensity of the surface urban heat island (SUHI) for the winter months was calculated at a diurnal scale for Kolkata from the fixed urban surface for various rural landscapes. The mean intensity of SUHI reveals a strong diurnal variation where the positive higher values (5.6 ˚C) occurred during nighttime, while negative and lower values (0.6 ˚C) were found during the daytime. Because Kolkata is a high-intensity urban area—it results in more pronounced heating effects during nighttime and greater heat retention during the daytime. Therefore, the UHI is typically viewed as a nighttime phenomenon in the KMA with intensity by nighttime warming over the Indian subcontinent. This is because the surface temperature of thermally induced building masses is warmer at nighttime as heat is released slower than in surrounding rural areas.

The city scale implementation of SCMs leads to modifying the local meteorological conditions. The higher level of buoyancy effects of an undiluted air parcel connected to the potential updraft strength of vertical convection substantially decreased during the stable cold night over the city where SCMs are applied. The situation depends on whether the wet-adiabatic process is deemed reversible or irreversible and whether the latent heat of freezing is considered over the city with SCMs. Due to the lack of convective available potential energy (CAPE) during winter in cities with SCMs, the environment is in hydrostatic balance. The pressure of the parcel is identical to that of the environment. Overall, the planetary boundary layer (PBL) starts rising on the south-facing slopes and near the ridges (warmed up by sun first and not hindered by pockets of cold air accumulated down the valley overnight) and becomes more spatially homogeneous during the afternoon to nighttime. Temporally, the convection ends around the early evening. The lower atmosphere then starts dissipating, and the plain circulation starts reversing into a sinking motion. There is an inadequate residual layer at nighttime since advection by the synoptic wind system dominates from the nearby southern sea and northern long-range mountain or surrounding suburbs.

SCMs create regional "high pressure" air envelop over the urban domain. It can be seen in the near-surface wind, which is considerably reduced during the daytime up to 4–6 ms^{-1}. The apparent consequence of the input heat deficit is the reduction of ambient temperature over the urban domain. Moreover, the offset of input solar radiation reveals a light energy source to develop the urban atmospheric mixing layer during the urban atmosphere's winter. The simulated results for Kolkata show that the constantly lower temperature could create an inversion layer near the surface when implementing SCMs, presented by the potential temperature with a vertical profile for the boundary layer

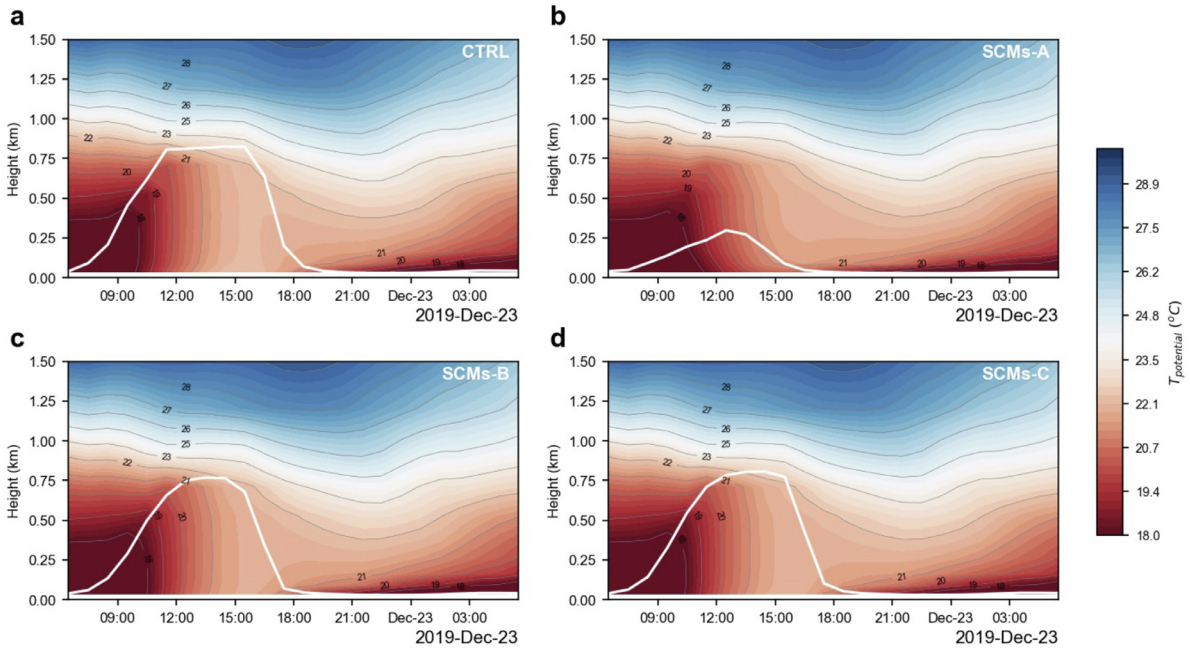

Fig. 5. Change in time of potential temperature over an urban area. Impacts of SCMs cooling on boundary layer stability can be evaluated through potential temperature for a diurnal cycle. During peak hours, the convective boundary layer developed the fastest way and gradually deeper with (a) CTRL compared to (b) SCMs-A, (c) SCMs-B, (d) SCMs-C in the lower atmosphere. Due to SCMs cooling, the PBL tends to be lower in thickness (white line), reducing the vertical wind speeds during daylight. In turn, this effect led to lesser vertical convective mixing and a lower PBL height. In other words, the PBL also contracts due to a reduction of rising thermals from the surface at nighttime.

(Fig. 5). These meteorological changes in the lower atmosphere could lead to a buildup of stagnant air over the urban environment. As a result, building heat remains poised over a city, preventing its easy rejection to space, resulting in the heating effects during night in the winter seasons as usual with SCMs as with the CTRL.

Discussion

SCMs in winter seasons

The minimum temperature of Indian cities during winter seasons substantially increased compared to previous decades. Although it is crucial to study means of passively reducing the heat trapped in the urban fabrics, it is as important to determine the unwanted side effects of these mitigation technologies.

This research has studied the effects of the implementation of SCMs during winter to determine the overcooling penalty at a city scale. All the materials were tested against a CTRL in Kolkata tropical wet and dry climate. The WRF-SLUCM model proved to simulate the city behavior accurately. The simulations results show that the implementation of different SCMs over the city of Kolkata led to a significant change in the thermal balance and influenced the lower atmosphere, creating an inversion layer at night.

All the SCMs were able to reduce the net inflow radiation, the more reflective and emissive the materials were, the more significant the drop in heat fluxes was. The maximum decrease of sensible heat, latent heat and net radiation occurred at peak hour, the more reflective and emissive scenario, SCMs-A, achieved mean values during the day of −86.7 Wm^{-2}, 18.1 Wm^{-2} and 161 Wm^{-2}, respectively. The SCMs had a very high impact on the decrease of the ambient, surface, roof and canopy, temperatures, with mean values up to 2.8 °C, 4.7 °C, 10.2 °C and 6 °C, respectively.

Moreover, the resulting lower temperatures in the city can develop an inversion layer, which could derive in nighttime heating effects due to the expansion of stagnant air.

Potential ways to overcome the overcooling

Passive radiative cooling devices present the highest potential to decrease the cooling needs of the built environment and counterbalance urban warming [8, 60]. Nevertheless, its application inevitably causes the increase of heating demand in winter, especially in cold climates, offsetting some of the cooling benefits. Although the overcooling during the winter in Kolkata was substantial, the penalty might be compensated by refrigeration savings during the summer. Colder climates might need more stringent solutions to alleviate the overcooling effect. To do so, SCMs might need to incorporate materials to adaptively control the optical properties, altering the heating or cooling power. This dynamic modulation can be achieved by thermochromic materials [21, 44], electrochromic materials [28], wet/dry chromism [36], or optical gratings [63].

With the emissivity changing with temperature, thermochromic materials, such as vanadium dioxide (VO_2), have been among the most promising candidates as adaptive radiative coolers. VO_2 can spontaneously change from metal to insulator at 68 °C, and this transition temperature is the closest to room temperature [61]. When applied to radiative coolers, a detailed demonstration of its effectiveness was presented [61]. A thin film maintained an almost constant temperature; it combined a radiative cooling film based on silicon monoxide and a vanadium dioxide thermochromic layer doped with tungsten [59]. The challenges for the synthesis of VO_2 are related to the coexistence of the various oxide forms and various polymorphs [18].

An asymmetric Fabry-Perot emitter was theoretically proposed with a lossless dielectric spacer inserted between a VO_2 thin film and an opaque aluminum substrate [58]; two differentiated behaviors were presented, the radiative power rose from 56 Wm^{-2} at 341 K and to 365 Wm^{-2} at 345 K. A multilayered device comprised of a vanadium dioxide thin film on a silicon substrate with a gold back reflector, demonstrated that switching could reduce the thermal fluctuations by up to a factor of two [40].

Similarly, the optical properties of electrochromic materials can change when energized by an electrical current. For example, when

$Li_4Ti_5O_{12}$ was lithiated to $Li_7Ti_{15}O_{12}$, the broadband emissivity in infrared increased [35]. In addition, both solar heating and radiative cooling under different daytime and nighttime skies were demonstrated. Under sunlight, a large tunable temperature range (18 °C) and sub-ambient around 4 °C can be attained.

Wet/dry chromism of some porous polymer coatings (PPCs) can also be used as an inexpensive paradigm for dynamic control of light and heat as their solar and infrared transmittance can change once wetted by a specific liquid [36]. For example, white poly (vinylidene fluoride-co-hexafluoropropylene) (P(VdF-HFP)) PPCs become transparent if wetted by fluids with a matched refractive index like isopropanol. Furthermore, being reversible, this transmittance modulation can be used for diurnal or seasonal thermoregulation.

The asymmetric electromagnetic transmission (AEMT) can be another potential modulator [63]. It permits outgoing radiative transmission but reflects incoming radiation of the same wavelengths. It was initially designed to limit the strong absorption of the additional heat load, thereby preventing the cooling capacity drops in a humid environment. If this material is turned upside down, it can be used in winter to prevent infrared emission but retain the absorption, facilitating the winter heating effect. However, this AEMT window has not been fabricated and experimentally tested.

Overall, regardless of the specific modulating mechanism and tunability, the cost of the manufacture and the feasibility of large-scale practical application remain the major challenge for the implementation of modulation techniques to SCMs.

Conclusion

Daytime radiative coolers or SCMs are among the most promising heat mitigation strategies, especially for cities with heat islands. Although the success of these materials is currently caught up by scalability, cost-effectiveness, and durability, they could play an essential role in aiding towards achieving thermal comfort during the cooling demanding periods. However, besides SCMs development limitations, they present a drawback when applied as passive elements during the heating seasons due to their overcooling potential.

For the first time, this research has studied the overcooling penalty of several SCMs scenarios during winter (heat demanding season) in the KMA. We simulated very efficient broadband SCMs, which can easily be run by a mesoscale climate model for large-scale testing. The simulations results revealed that there is substantial overcooling with SCMs for tropical winter seasons. Thus, the following conclusions can be obtained:

a) The broad implementation of SCMs can lower the city temperatures and decrease thermal comfort in winter.
b) The overcooling penalty might be up to 186 Wm^{-2} during the daytime.
c) In the most reflective scenario, the mean ambient temperature decrease was 2.8 °C and 1.5 °C during the day and night, respectively.
d) Reflective materials can change the lower atmosphere leading to inversion phenomena, resulting in heating effects during winter nights.

Future work is ongoing to expand and generalize the results of the case studies discussed here to include a wide array of cases in different climates, allowing a more substantial number of temperate-sector points to be considered in cold season severe weather environments. Moreover, the inclusion of modulation techniques such as the ones briefly discussed could reduce the unwanted overcooling penalty during the winter months while benefiting from the mitigating effects during the summer months.

Author contribution

AK, QVD, and SK designed and ran numerical simulations with the WRF model and analyzed the simulated results. RK helped with the data curation for WRF model. The manuscript was written by AK, LC, JF and, with revisions from all authors. MS coordinated and supervised the whole research.

Data availability

The data that support the findings of this study are available from the corresponding author upon reasonable request.

Code availability

The source code of WRF model Version 4.0 used in this paper can be downloaded from https://www2.mmm.ucar.edu/wrf/users/download/get_sources.html#current. Codes used to set up model simulations, analyze data, and create figures can be provided upon request from the corresponding author.

Declaration of Competing Interest

The authors declare no competing interests.

Acknowledgments

The authors would like to acknowledge the National Centers for Environmental Prediction (NCEP) and the Research Data Archive of the University Corporation for Atmospheric Research (RDA/UCAR) for providing the data.

References

[1] H. Akbari, S. Bretz, D.M. Kurn, J. Hanford, Peak power and cooling energy savings of high-albedo roofs, Energy Build 25 (1997) 117–126, doi:10.1016/S0378-7788(96)01001-8.
[2] H. Akbari, C. Cartalis, D. Kolokotsa, A. Muscio, A.L. Pisello, F. Rossi, M. Santamouris, A. Synnefa, N.H. Wong, M. Zinzi, Local climate change and urban heat island mitigation techniques – the state of the art, J. Civ. Eng. Manag. 22 (2016) 1–16, doi:10.3846/13923730.2015.1111934.
[3] A. Baniassadi, D.J. Sailor, G.A. Ban-Weiss, Potential energy and climate benefits of super-cool materials as a rooftop strategy, Urban Clim 29 (2019) 100495, doi:10.1016/j.uclim.2019.100495.
[4] C. Bartesaghi-Koc, S. Haddad, G. Pignatta, R. Paolini, D. Prasad, M. Santamouris, Can urban heat be mitigated in a single urban street? Monitoring, strategies, and performance results from a real scale redevelopment project, Sol. Energy 216 (2021) 564–588, doi:10.1016/j.solener.2020.12.043.
[5] J.P. Bijarniya, J. Sarkar, P. Maiti, Environmental effect on the performance of passive daytime photonic radiative cooling and building energy-saving potential, J. Clean. Prod. 123119 (2020), doi:10.1016/j.jclepro.2020.123119.
[6] S. Boixo, M. Diaz-Vicente, A. Colmenar, M.A. Castro, Potential energy savings from cool roofs in Spain and Andalusia, Energy 38 (2012) 425–438, doi:10.1016/j.energy.2011.11.009.
[7] L. Carlosena, Á. Andueza, L. Torres, O. Irulegi, R.J. Hernández-Minguillón, J. Sevilla, M. Santamouris, Experimental development and testing of low-cost scalable radiative cooling materials for building applications, Sol. Energy Mater. Sol. Cells 230 (2021) 111209, doi:10.1016/j.solmat.2021.111209.
[8] L. Carlosena, Á. Ruiz-Pardo, J. Feng, O. Irulegi, R.J. Hernández-Minguillón, M. Santamouris, On the energy potential of daytime radiative cooling for urban heat island mitigation, Sol. Energy 208 (2020) 430–444, doi:10.1016/j.solener.2020.08.015.
[9] F. Chen, J. Dudhia, Coupling an advanced land surface–hydrology model with the Penn State–NCAR MM5 modeling system. Part I: model implementation and sensitivity, Mon. Weather Rev. 129 (2001) 569–585 https://doi.org/10.1175/1520-0493(2001)129<0569:CAALSH>2.0.CO;2.
[10] A. De Gracia, L. Navarro, A. Castell, Á. Ruiz-Pardo, S. Álvarez, L.F. Cabeza, Thermal analysis of a ventilated facade with PCM for cooling applications, Energy Build 65 (2013) 508–515, doi:10.1016/j.enbuild.2013.06.032.
[11] J. Dudhia, Numerical Study of Convection Observed during the Winter Monsoon Experiment Using a Mesoscale Two-Dimensional Model, J. Atmospheric Sci. 46 (1989) 3077–3107 https://doi.org/10.1175/1520-0469(1989)046<3077:NSOCOD>2.0.CO;2.
[12] R. Family, M.P. Mengüç, Materials for Radiative Cooling: a Review, in: Procedia Environ. Sci., Sustainable synergies from Buildings to the Urban Scale, 38, 2017, pp. 752–759, doi:10.1016/j.proenv.2017.03.158.
[13] J. Feng, K. Gao, M. Santamouris, K.W. Shah, G. Ranzi, Dynamic impact of climate on the performance of daytime radiative cooling materials, Sol. Energy Mater. Sol. Cells 208 (2020) 110426, doi:10.1016/j.solmat.2020.110426.
[14] J. Feng, A. Khan, Q.-V. Doan, K. Gao, M. Santamouris, The heat mitigation potential and climatic impact of super-cool broadband radiative coolers on a city scale, Cell Rep. Phys. Sci. 2 (2021) 100485, doi:10.1016/j.xcrp.2021.100485.

[15] D. Founda, M. Santamouris, Synergies between Urban Heat Island and Heat Waves in Athens (Greece), during an extremely hot summer (2012), Sci. Rep. 7 (2017), doi:10.1038/s41598-017-11407-6.

[16] S. Garshasbi, S. Huang, J. Valenta, M. Santamouris, Can quantum dots help to mitigate urban overheating? An experimental and modelling study, Sol. Energy 206 (2020) 308–316, doi:10.1016/j.solener.2020.06.010.

[17] E.A. Goldstein, A.P. Raman, S. Fan, Sub-ambient non-evaporative fluid cooling with the sky, Nat. Energy 2 (2017) nenergy2017143, doi:10.1038/nenergy.2017.143.

[18] C. Granqvist, G. Niklasson, Thermochromic oxide-based thin films and nanoparticle composites for energy-efficient glazings, Buildings 7 (2016) 3, doi:10.3390/buildings7010003.

[19] Z. Huang, X. Ruan, Nanoparticle embedded double-layer coating for daytime radiative cooling, Int. J. Heat Mass Transf. 104 (2017) 890–896, doi:10.1016/j.ijheatmasstransfer.2016.08.009.

[20] IPCCClimate change 2021: the physical science basis. contribution of working group I to the sixth assessment report of the intergovernmental panel on climate change, Intergovernmental Panel on Climate Change, 2021.

[21] H. Ji, D. Liu, H. Cheng, C. Zhang, L. Yang, Vanadium dioxide nanopowders with tunable emissivity for adaptive infrared camouflage in both thermal atmospheric windows, Sol. Energy Mater. Sol. Cells 175 (2018) 96–101, doi:10.1016/j.solmat.2017.10.013.

[22] J.S. Kain, The Kain–Fritsch Convective Parameterization: an Update, J. Appl. Meteorol. Climatol. 43 (2004) 170–181 https://doi.org/10.1175/1520-0450(2004)043<0170:TKCPAU>2.0.CO;2.

[23] T. Karlessi, M. Santamouris, K. Apostolakis, A. Synnefa, I. Livada, Development and testing of thermochromic coatings for buildings and urban structures, Sol. Energy 83 (2009) 538–551, doi:10.1016/j.solener.2008.10.005.

[24] D.– D. Kolokotsa, G. Giannariakis, K. Gobakis, G. Giannarakis, A. Synnefa, M. Santamouris, Cool roofs and cool pavements application in Acharnes, Greece. Sustain. Cities Soc. 37 (2018) 466–474, doi:10.1016/j.scs.2017.11.035.

[25] D. Kolokotsa, M. Santamouris, S.C. Zerefos, Green and cool roofs' urban heat island mitigation potential in European climates for office buildings under free floating conditions, Sol. Energy 95 (2013) 118–130, doi:10.1016/j.solener.2013.06.001.

[26] I. Kousis, C. Fabiani, L. Gobbi, A.L. Pisello, Phosphorescent-based pavements for counteracting urban overheating – A proof of concept, Sol. Energy 202 (2020) 540–552, doi:10.1016/j.solener.2020.03.092.

[27] H. Kusaka, H. Kondo, Y. Kikegawa, F. Kimura, A simple single-layer urban canopy model for atmospheric models: comparison with multi-layer and slab models, Bound.-Layer Meteorol 101 (2001) 329–358, doi:10.1023/A:1019207923078.

[28] F. Lang, H. Wang, S. Zhang, J. Liu, H. Yan, Review on variable emissivity materials and devices based on smart chromism, Int. J. Thermophys. 39 (2017) 6, doi:10.1007/s10765-017-2329-0.

[29] A. Leroy, B. Bhatia, C.C. Kelsall, A. Castillejo-Cuberos, M.D.C. H, L. Zhao, L. Zhang, A.M. Guzman, E.N. Wang, High-performance subambient radiative cooling enabled by optically selective and thermally insulating polyethylene aerogel, Sci. Adv. 5 (2019) eaat9480, doi:10.1126/sciadv.aat9480.

[30] W. Li, S. Fan, Nanophotonic control of thermal radiation for energy applications [Invited], Opt. Express 26 (2018) 15995, doi:10.1364/OE.26.015995.

[31] W. Li, Y. Shi, Z. Chen, S. Fan, Photonic thermal management of coloured objects, Nat. Commun. 9 (2018), doi:10.1038/s41467-018-06535-0.

[32] Y.-.L. Lin, R.D. Farley, H.D. Orville, Bulk parameterization of the snow field in a cloud model, J. Appl. Meteorol. Climatol. 22 (1983) 1065–1092 https://doi.org/10.1175/1520-0450(1983)022<1065:BPOTSF>2.0.CO;2.

[33] H. Luo, J. Wu, Effects of urban growth on the land surface temperature: a case study in Taiyuan, China, Environ. Dev. Sustain. 23 (2021) 10787–10813, doi:10.1007/s10668-020-01087-0.

[34] E. Malek, Evaluation of effective atmospheric emissivity and parameterization of cloud at local scale, Atmospheric Res 45 (1997) 41–54, doi:10.1016/S0169-8095(97)00020-3.

[35] J. Mandal, S. Du, M. Dontigny, K. Zaghib, N. Yu, Y. Yang, Li4Ti5O12: a visible-to-infrared broadband electrochromic material for optical and thermal management, Adv. Funct. Mater. 28 (2018) 1802180, doi:10.1002/adfm.201802180.

[36] J. Mandal, M. Jia, A. Overvig, Y. Fu, E. Che, N. Yu, Y. Yang, Porous polymers with switchable optical transmittance for optical and thermal regulation, Joule, 2019, doi:10.1016/j.joule.2019.09.016.

[37] G.L. Mellor, T. Yamada, A hierarchy of turbulence closure models for planetary boundary layers, J. Atmos. Sci. 31 (1974) 1791–1806.

[38] E.J. Mlawer, S.J. Taubman, P.D. Brown, M.J. Iacono, S.A. Clough, Radiative transfer for inhomogeneous atmospheres: RRTM, a validated correlated-k model for the longwave, J. Geophys. Res. Atmospheres 102 (1997) 16663–16682, doi:10.1029/97JD00237.

[39] A.K. Moridani, R. Zando, W. Xie, I. Howell, J.J. Watkins, .J..-H. Lee, Plasmonic thermal emitters for dynamically tunable infrared radiation, Adv. Opt. Mater. 5 (2017) 1600993, doi:10.1002/adom.201600993.

[40] A.M. Morsy, M.T. Barako, V. Jankovic, V.D. Wheeler, M.W. Knight, G.T. Papadakis, L.A. Sweatlock, P.W.C. Hon, M.L. Povinelli, Experimental demonstration of dynamic thermal regulation using vanadium dioxide thin films, Sci. Rep. 10 (2020) 13964, doi:10.1038/s41598-020-70931-0.

[41] J.N. Munday, Tackling climate change through radiative cooling, Joule, 2019 0, doi:10.1016/j.joule.2019.07.010.

[42] A. Nurwanda, T. Honjo, The prediction of city expansion and land surface temperature in Bogor City, Indonesia, Sustain. Cities Soc. 52 (2020) 101772, doi:10.1016/j.scs.2019.101772.

[43] T.R. Oke, G.T. Johnson, D.G. Steyn, I.D. Watson, Simulation of surface urban heat islands under 'ideal' conditions at night part 2: diagnosis of causation, Bound.-Layer Meteorol 56 (1991) 339–358, doi:10.1007/BF00119211.

[44] M. Ono, K. Chen, W. Li, S. Fan, Self-adaptive radiative cooling based on phase change materials, Opt. Express 26 (2018) A777, doi:10.1364/OE.26.00A777.

[45] G. Perez, V.R. Allegro, M. Corroto, A. Pons, A. Guerrero, Smart reversible thermochromic mortar for improvement of energy efficiency in buildings, Constr. Build. Mater. 186 (2018) 884–891, doi:10.1016/j.conbuildmat.2018.07.246.

[46] J.E. Pleim, A combined local and nonlocal closure model for the atmospheric boundary layer. Part I: model description and testing, J. Appl. Meteorol. Climatol. 46 (2007) 1383–1395, doi:10.1175/JAM2539.1.

[47] A.P. Raman, M.A. Anoma, L. Zhu, E. Rephaeli, S. Fan, Passive radiative cooling below ambient air temperature under direct sunlight, Nature 515 (2014) 540–544, doi:10.1038/nature13883.

[48] K.K. Roman, T. O'Brien, J.B. Alvey, O. Woo, Simulating the effects of cool roof and PCM (phase change materials) based roof to mitigate UHI (urban heat island) in prominent US cities, Energy 96 (2016) 103–117, doi:10.1016/j.energy.2015.11.082.

[49] A. Salvati, M. Kolokotroni, in: Impact of urban albedo on microclimate and thermal comfort over a heat wave event in London, WINDSOR, 2020, p. 14.

[50] M. Santamouris, Recent progress on urban overheating and heat island research. Integrated assessment of the energy, environmental, vulnerability and health impact. Synergies with the global climate change, Energy Build 207 (2020) 109482, doi:10.1016/j.enbuild.2019.109482.

[51] M. Santamouris, Regulating the damaged thermostat of the cities—Status, impacts and mitigation challenges, Energy Build 91 (2015) 43–56, doi:10.1016/j.enbuild.2015.01.027.

[52] M. Santamouris, C. Cartalis, A. Synnefa, D. Kolokotsa, On the impact of urban heat island and global warming on the power demand and electricity consumption of buildings—A review, Energy Build. Renew. Energy Sour. Health. Build. 98 (2015) 119–124, doi:10.1016/j.enbuild.2014.09.052.

[53] M. Santamouris, J. Feng, Recent progress in daytime radiative cooling: is it the air conditioner of the future? Buildings 8 (2018) 168, doi:10.3390/buildings8120168.

[54] M. Santamouris, F. Fiorito, On the impact of modified urban albedo on ambient temperature and heat related mortality, Sol. Energy 216 (2021) 493–507, doi:10.1016/j.solener.2021.01.031.

[55] M. Santamouris, P. Osmond, Increasing green infrastructure in cities: impact on ambient temperature, air quality and heat-related mortality and morbidity, Buildings 10 (2020) 233, doi:10.3390/buildings10120233.

[56] M. Santamouris, G.Y. Yun, Recent development and research priorities on cool and super cool materials to mitigate urban heat island, Renew. Energy 161 (2020) 792–807, doi:10.1016/j.renene.2020.07.109.

[57] L.H. Schinasi, T. Benmarhnia, A.J. De Roos, Modification of the association between high ambient temperature and health by urban microclimate indicators: a systematic review and meta-analysis, Environ. Res. 161 (2018) 168–180, doi:10.1016/j.envres.2017.11.004.

[58] S. Taylor, Y. Yang, L. Wang, Vanadium dioxide based Fabry-Perot emitter for dynamic radiative cooling applications, J. Quant. Spectrosc. Radiat. Transf. 197 (2017) 76–83, doi:10.1016/j.jqsrt.2017.01.014.

[59] M. Tazawa, P. Jin, S. Tanemura, Thin film used to obtain a constant temperature lower than the ambient, Thin Solid Films 281–282 (1996) 232–234, doi:10.1016/0040-6090(96)08620-8.

[60] G. Ulpiani, G. Ranzi, J. Feng, M. Santamouris, Expanding the applicability of daytime radiative cooling: technological developments and limitations, Energy Build 243 (2021) 110990, doi:10.1016/j.enbuild.2021.110990.

[61] G. Ulpiani, G. Ranzi, K.W. Shah, J. Feng, M. Santamouris, On the energy modulation of daytime radiative coolers: a review on infrared emissivity dynamic switch against overcooling, Sol. Energy 209 (2020) 278–301, doi:10.1016/j.solener.2020.08.077.

[62] E. Vardoulakis, D. Karamanis, A. Fotiadi, G. Mihalakakou, The urban heat island effect in a small Mediterranean city of high summer temperatures and cooling energy demands, Sol. Energy 94 (2013) 128–144, doi:10.1016/j.solener.2013.04.016.

[63] R.Y.M. Wong, C.Y. Tso, C.Y.H. Chao, B. Huang, M.P. Wan, Ultra-broadband asymmetric transmission metallic gratings for subtropical passive daytime radiative cooling, Sol. Energy Mater. Sol. Cells 186 (2018) 330–339, doi:10.1016/j.solmat.2018.07.002.

[64] X. Xue, M. Qiu, Y. Li, Q.M. Zhang, S. Li, Z. Yang, C. Feng, W. Zhang, J.-.G. Dai, D. Lei, W. Jin, L. Xu, T. Zhang, J. Qin, H. Wang, S. Fan, Creating an Eco-Friendly Building Coating with Smart Subambient Radiative Cooling, Adv. Mater. (2020) 1906751 n/a, doi:10.1002/adma.201906751.

[65] Y. Yang, Y. Zhang, Passive daytime radiative cooling: principle, application, and economic analysis, MRS Energy Sustain 7 (2020) E18, doi:10.1557/mre.2020.18.

[66] M. Zeyghami, D.Y. Goswami, E. Stefanakos, A review of clear sky radiative cooling developments and applications in renewable power systems and passive building cooling, Sol. Energy Mater. Sol. Cells 178 (2018) 115–128, doi:10.1016/j.solmat.2018.01.015.

[67] B. Zhao, M. Hu, X. Ao, N. Chen, G. Pei, Radiative cooling: a review of fundamentals, materials, applications, and prospects, Appl. Energy 236 (2019) 489–513, doi:10.1016/j.apenergy.2018.12.018.

[68] S. Zheng, Y. Xu, Q. Shen, H. Yang, Preparation of thermochromic coatings and their energy saving analysis, Sol. Energy 112 (2015) 263–271, doi:10.1016/j.solener.2014.09.049.